ChemComm

Accepted Manuscript

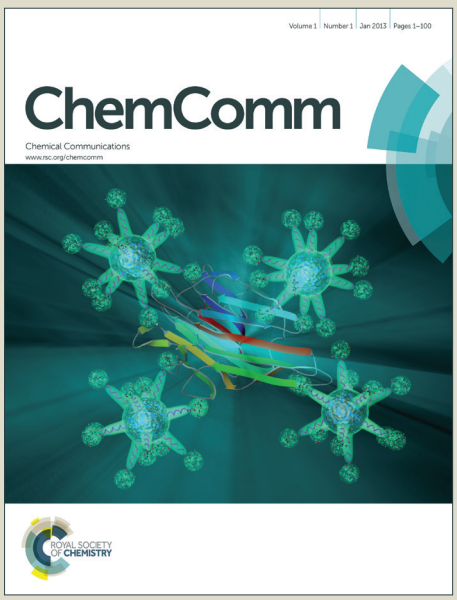

ROYAL SOCIETY OF CHEMISTRY

www.rsc.org/chemcomm

Chem. Commun.

RSCPublishing

COMMUNICATION

Tailor-made graphite oxide-DAB poly(propylene imine) dendrimer intercalated hybrids and their potential for efficient CO_2 adsorption

Cite this: DOI: 10.1039/x0xx00000x

Received 00th January 2012,
Accepted 00th January 2012

DOI: 10.1039/x0xx00000x

www.rsc.org/

T. Tsoufis,[a*] F. Katsaros,[a] Z. Sideratou,[a] G. Romanos,[a] O. Ivashenko,[b] P. Rudolf,[b] B.J. Kooi,[b,c] S. Papageorgiou,[a] and M.A. Karakassides.[d]

We report the rational design and synthesis of DAB poly(propylene imine) dendrimer (DAB) intercalated graphite oxide (GO) hybrids with tailorable interlayer distances. The amine groups originating from the intercalated dendrimer molecules cross-link adjacent GO sheets and strongly favour CO_2 adsorption under wet flue gas conditions.

Graphene has emerged as an exciting two-dimensional material possessing many unique properties including a very high surface area (>2.500 cm^2/gr).[1a] A very attractive chemical derivative of graphene is graphene oxide, which also exhibits a two-dimensional structure, but unlike pristine graphene, which is build up exclusively from carbon atoms, graphene oxide sheets are decorated with oxygen containing groups (mainly epoxide, hydroxyl, carbonyl and carboxyl groups) as a result of the preparation method (oxidative treatment of graphite).[1b] On the other hand, dendrimers are a very versatile family of tailor-made polymers with distinct size and shape. These highly ordered hyperbranched macromolecules of low polydispersity, exhibit a well-defined number of active functional groups distributed along their branches and periphery. Until now the field of graphene-dendrimer hybrids has been little explored. Up to date, literature reports involve mainly the use of *high* molecular weight (generation) polyamidoamine (PAMAM) dendrimers towards the covalent chemical surface functionalization of GO.[2a,b,c]

Instead, we propose the use of *low* molecular weight (MW) DAB dendrimers for which the incorporation within the interlayer space of GO is less demanding because their dendritic structures are of smaller size. The reduced dimension of the selected DAB guest allows to preserve the parallel arrangement of the GO sheets when it is inserted in the interlayer space of GO host to create a pillared structure as illustrated in Scheme 1. We intercalated DAB_4, DAB_8, DAB_{16} dendrimers (of MW=300, 741 and 1.622 Da respectively) into the interlayer space of GO without the aid of any coupling agent. Powder X-ray diffraction (PXRD) allows the precise determination of the d_{001} spacing via the Bragg law. The PXRD patterns of GO after reaction with the various DAB dendrimers (Fig 1,b,c,d left) revealed a significant shift of the [001] diffraction peak compared to pristine GO (Fig. 1,a left). The corresponding increased d_{001} spacing unequivocally testifies to the successful insertion of the guest DAB into the interlayer space of the layered host.

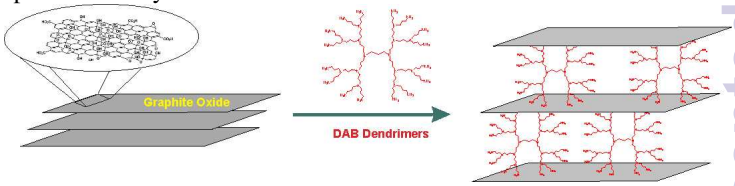

Scheme 1 Schematic representation of the synthetic approach.

The resulting d_{001} values scale with the size of the DAB, in particular, GO intercalated with DAB_4 ($GO\text{-}DAB_4$) showed a [001] diffraction peak at 2θ=8.3° corresponding to a *d*-spacing of 8.5 Å, while for $GO\text{-}DAB_8$ and $GO\text{-}DAB_{16}$ *d*-spacings of 13.6 (further confirmed by HRTEM images, Fig. S6c, ESI) and 15.9 Å, respectively were determined.

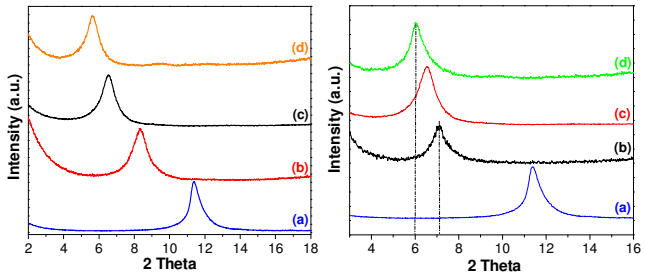

Fig. 1 PXRD patterns (recorded using a Cu Ka source, λ=0.15418 nm) of pristine GO (a) and (*Left*) various GO-DAB hybrids; $GO\text{-}DAB_4$ (b), $GO\text{-}DAB_8$ (c), and $GO\text{-}DAB_{16}$, (*Right*) $GO\text{-}DAB_8$ samples for various $GO:DAB_8$ (wt/wt) loadings; 1:0.5 (b), 1:3 (c), and 1:10 (d).

We also demonstrated that such intercalated structures can only be achieved with low MW DAB intercalation into GO. In fact, we also reacted pristine GO with a significantly higher MW DAB (DAB_{64}, MW=7.200 Da) under the same experimental conditions. In this case, the hyperbranched DAB structure is too large to be accommodated within the interlayer space of GO, resulting in the loss of the GO's sheets parallel conformation. The PXRD pattern of the $GO\text{-}DAB_{64}$ (Fig. S1,

ESI), lacks a noticeable diffraction peak at low 2θ values, pointing to a disordered arrangement of the GO sheets and to an exfoliated GO-DAB hybrid.

We also evaluated the effect of increasing DAB loading in the GO interlayer space by employing different reacting weight ratios between GO and DAB_8. The PXRD patterns (Fig. 1,b,c,d *right*), of the GO-DAB_8 hybrids after reacting 1:0.5, 1:3 and 1:10 weight ratios of GO:DAB_8, showed d_{001} values of respectively 12.3, 13.6, and 14.8 Å. These results clearly point to a trend where the basal spacing of intercalated GO-DAB_8 samples augments with increasing DAB_8 loading. This increase is attributed to different configurations adopted by intercalated DAB_8 molecules within the GO interlayer space.[2d]

As previously suggested for the intercalation reactions of GO with various bi-functional molecules,[2c] their reaction with the layered host can occur "intra-molecularly" (when the intercalated molecule reacts with two reactive sites at the same GO layer) forming "rings" or "inter-molecularly" (when the reaction takes place between reactive sites located on two different GO layers) forming "bridges". Swelling experiments have been reported[3] as additional proof for the existence of covalent cross-links ("bridges") between adjacent layers. If successful 'bridging' occurs between adjacent sheets, the resulting cross-linked structures should resist further swelling. We tested this with PXRD measurements performed after a sequential intercalation reaction for one of the GO-DAB hybrids. In detail, we reacted the as-prepared GO-DAB_8 (1:3 ratio) hybrid with a long, linear amine (*n*-dodecylamine) and found that the PXRD pattern of the GO-DAB_8-dodecylamine sample (Fig. S2b, ESI) did not reveal any significant shifting of the 001 diffraction peak. This is different from previously reported[3,4] proof-of-concept experiments, which involved the initial intercalation reaction of a *mono*-functional amine (n-butylamine) into GO, followed by the sequential reaction with dodecylamine and where PXRD analysis showed that the interlayer distance of the butylamine intercalated GO was further increased after reacting with dodecylamine, suggesting the expansion of an unconstrained system along the *c*-axis and therefore "intra-molecular" bonding.[3,4] Therefore, for GO-DAB, the lack of additional swelling is a further strong evidence of the cross-linking between the GO sheets by DAB_8.

Additional information regarding the chemical environment of the intercalated DAB_8 within the GO interlayer space was gathered from X-ray photoelectron spectroscopy (XPS) measurements. The XPS survey spectra of the pristine GO and the intercalated GO-DAB_8 (1:3 ratio) (Fig. S3a,b, ESI) exhibit the characteristic O1*s* and C1*s* contributions from the GO graphitic framework; the spectrum of GO-DAB_8 comprises an additional peak centred at a binding energy of ~400 eV, characteristic for Nitrogen. This contribution appears also in the reference survey spectrum of pure DAB_8 (Fig. S3c, ESI) and its appearance in the spectrum of GO-DAB_8 therefore clearly highlights the presence of the nitrogen-rich DAB_8 in the final hybrid.

Further information regarding the bonding of DAB_8 in the GO interlayer space can be gathered from the C1s core level XPS spectra. The C1*s* core line of pristine GO can be fitted using three components as presented in Fig. 2a. The lowest binding energy component at 284.5 eV is attributed to C=C and C-C bonds; a second peak at 286.6 eV is due to C-O bonds, while the component 288.5 eV is assigned to O-C=O bonds. The corresponding spectrum of GO-DAB_8 (1:3 ratio) also fitted using three components as presented in Fig. 2b, showed broadening and a significant increase in the intensity of the component at 286.6 eV, from 50% to 61% of the overall carbon intensity. This change is attributed to the introduction of additional C-N bonds originating both from DAB_8 structure as well as from newly formed C-N bonds as a result of the DAB_8 "grafting-to" the GO framework. A similar XPS fingerprint has been reported previously after successful covalent attachment of multi-amine molecules at the GO framework.[2a]

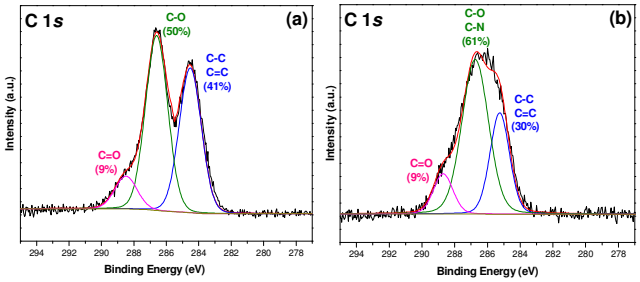

Fig. 2 Core-level XPS spectra and fit of the C1*s* region for pristine GO (*a*), and GO-DAB_8 (*b*).

The analysis of the chemical environment of nitrogen in GO-DAB_8 is of great importance as it illustrates the nature of the interactions between the GO sheets and the nitrogen containing groups of intercalated DAB_8. Therefore we also recorded the N1*s* core level spectrum of GO-DAB_8 (1:3 ratio) (Fig. 3a); the spectrum was fitted using three contributions. The lower binding energy peak at 399.5 eV, assigned to –C(O)-N- and/or –C=N- bonds, does not appear in the corresponding spectrum of pure DAB_8 (Fig 3c) and therefore testifies to the grafting of the amine containing DAB_8 chains onto the GO sheet. The second component at 400.7 eV, which accounts for 55% of the overall nitrogen intensity of the hybrid, was also observed in the corresponding spectrum of pure DAB_8, in agreement with previous XPS studies of DAB_8 molecules. The higher binding energy component of GO-DAB_8 (401.8 eV) is attributed to protonated amine groups,[4,5] mainly due to electrostatic interactions between the amine groups of DAB_8 and the negative carboxyl groups of GO.[6] These findings were further confirmed by FTIR studies (Fig. S4, ESI).

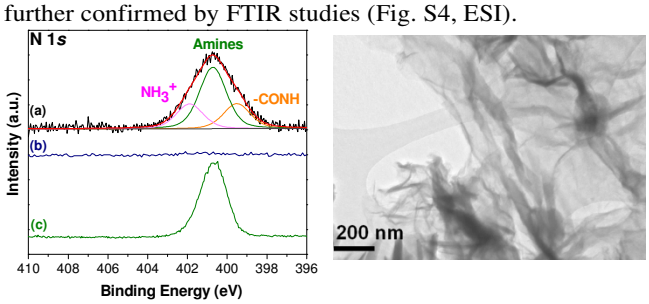

Fig. 3 (*Left)* N1s core-level XPS spectra and fit of GO-DAB_8 (a), pristine GO (b) and pure DAB_8 (c); (*Right*) TEM image of GO-DAB_8.

Taken together, the XPS and FTIR spectra suggest that the intercalation of DAB_8 into GO occurs mainly via a nucleophilic ring-opening reaction on the epoxy groups located on the graphitic framework of GO, as documented for reactions between GO and amino–containing molecules, and especially for intercalation reactions.[4,6,7] Furthermore, the appearance of an extra –C(O)-N- and/or -C=N- contribution (XPS N1*s* spectra), indicate that additional bonds are formed between the GO host and the intercalated DAB_8 derive from the reaction of C=O containing groups (GO) with the amino groups (DAB_8).[8]

Raman measurements provided insight into the structural order of the hybrid materials (Fig. S5, ESI). The relative ratio I_D/I_G, between the intensities of the D peak at ~1350 cm^{-1}, assigned to an

A_{1g} breathing mode activated by the relaxation of the Raman selection rule in the presence of defects, and the high frequency E_{2gn} Raman allowed optical phonon mode at ~1580 cm^{-1}, known as G peak,[9a] was increased from 0.93 for pristine GO, to 1.06, 1.17, and 1.26 for GO-DAB_4, GO-DAB_8 and GO-DAB_{16}, respectively. The recorded trend of I_D/I_G values reflects the increased disorder due to the nucleophilic addition of DAB's amino groups and the subsequent formation of covalent bonds, a phenomenon commonly reported in Raman studies of functionalized GO with "grafted-to" species.[9a]

The morphology of the synthesized materials was studied by scanning electron (SEM) and transmission electron (TEM) microscopies. Both SEM and TEM provided evidence for the occurrence of significant morphological changes resulting from DAB_8 intercalation. A representative TEM image of a GO-DAB_8 (1:3 ratio) presented in Fig.3 shows highly crumpled GO sheets rather than flat layered sheets as observed for pristine GO (compare with Fig. S6a,b, ESI). Similar morphological effects have been reported for successful intercalation of cross-linking agents into GO.[4,9b] Therefore, it seems reasonable to conclude that the intercalated DAB_8 molecules contributed to the roughness of the hybrids through their ability to react either intra- and/or inter-molecularly. Additional SEM measurements further supported this finding; SEM images of pristine GO (Fig. S7a,b, ESI) revealed a typical lamellar structure (flat surfaces), while GO-DAB showed randomly aggregated, thin, crumpled sheets loosely connected to one another (Fig. S7c,d, ESI).

The CO_2 adsorption capacity of GO-DAB_8 was studied employing the gravimetric technique and compared with the corresponding behaviour of pristine GO (Tables S1, S2). Although dry GO adsorbed higher amounts of CO_2 compared to dry GO-DAB_8 (Fig. S8, ESI), a significant enhancement of the CO_2 adsorption capacity (Table S2, Fig. S9b) and faster kinetics (Fig. S9c) were observed for the intercalated sample when pre-adsorbed water was involved (simulating flue gas conditions). In particular, wet GO-DAB_8 (1:3 ratio) reached the value of ~2 mmol g^{-1} (P/P_0=0.35)for ~30% DAB_8 loading (as calculated by elemental analysis- Table S3, ESI). This is among the highest values reported for CO_2 adsorption capacity on amine based hybrid organic-inorganic samples (at atmospheric pressure and 310 K).[10] Only in the exceptional case of polyethyleneimine (PEI), impregnated mesoporous carbon materials[11] (73% PEI loading on ultra-large mesopores), it has been reported adsorption capacity of 4.2 mmol g^{-1}. However, this value was achieved at higher temperatures (75 ^oC), while a decrease in both the adsorption capacity and the adsorption rate was observed under moist conditions. On the contrary, the intercalated GO-DAB_8 (1:3 ratio) under humid conditions exhibited improved adsorption amount (~3 times increase) and faster kinetics (3 times faster for 50% loading, ~6 times faster for 80% CO_2 adsorption) in regards to dry sample. The observed capacity under aqueous environment surpasses even that of ZIF-69 (1.7 mmol g^{-1}), which is currently considered as one of the most promising materials for CO_2 separation.[12]

The enhancement of the CO_2 adsorption in the case of the GO-DAB_8 (1:3 ratio) upon wetting is due to the presence of DAB's amino groups which can form carbamates through zwitterions (primary amines) and bicarbonates (tertiary amines).[13] The formation of these groups is readily facilitated in the presence of a base (hydroxyl groups of water). Additionally, water molecules can abstract protons from the zwitterions, making more NH_2 groups available for interaction with CO_2. On the other hand, the adsorbed water molecules on DAB_8 favour the formation of continuous liquid phase channels, which in turn increase the solubility of CO_2 in the liquid (H_2O) phase, thereby improving the adsorption kinetics.

In conclusion, we demonstrate the potential of a facile and versatile approach towards the bulk synthesis of DAB intercalated GO hybrids whose interlayer distances can be tailored by selecting different low molecular weight DAB dendrimers and/or by varying the DAB loading. Due to the increased *d*-distance and mainly due to the introduced active amine-groups, the resulting cross-linked GO-based hybrids display significant CO_2 adsorption upon wetting. In order to fully explore the CO_2 capture potential, further work on similar GO-based, hybrid systems synthesized using different amine-containing polymers (e.g. PEI) will be carried out.

This work was financially supported by EU under the FP7 PEOPLE-2012-IAPP-SANAD (No 324443), and PEOPLE-2011-IAPP-CARBONCOMP (No. 286413) projects. Additional support came from the "Top Research School" program of the Zernike Institute for Advanced Materials under the Bonus Incentive Scheme (BIS) of the Netherlands' Ministry of Education, Science, and Culture.

Notes and references

[a] NCSR "Demokritos", IAMPPNM, GR15310, Athens, Greece.
[b] Zernike Institute for Advanced Materials, University of Groningen, Nijenborgh 4, NL9747AG Groningen, The Netherlands.
[c] Materials innovation institute M2i, University of Groningen, Nijenborgh 4, NL9747AG Groningen, The Netherlands.
[d] Department of Materials Science and Engineering, University of Ioannina, GR45110 Ioannina, Greece.

Electronic Supplementary Information (ESI) available: PXRD, XPS, FTIR, RAMAN, SEM, (HR-)TEM, TGA, elemental analysis and CO_2 adsorption data and experimental details. See DOI: 10.1039/c000000x/

1 (a) R. Kumar, V.M. Suresh, T.K. Maji and C.N.R. Rao, *Chem. Commun.* 2014, **50**, 2015; (b) D.R. Dreyer, S. Park, C.W. Bielawski and R.S. Ruoff, *Chem. Soc. Rev.* 2010, **1**, 228.
2 (a) J.M. Kim, J. Kim and J. Kim, *Chem. Commun.* 2012, **48**, 9233; (b) F. Zhao, W. Li, *J. Mater. Chem.,* 2012, **22**, 3082; (c) Z. Luo, L. Yuwen, Y. Hana, J. Tiana, X. Zhua, L. Weng, L. Wang, *Biosens. Bioelectron.* 2012, **36**, 179; (c) H. He, T. Riedl, A. Lerf, and J. Klinowski, *J. Phys. Chem.* 1996, **100**, 19954; (d) I. Tsogas, D. Tsiourvas, G. Nounesis, and C. Paleos, *Langmuir* 2006, **22**, 11322.
3 M. Herrera-Alonso, A.A. Abdala, M.J. McAllister, I.A. Aksay, and R.K. Prud'homme, *Langmuir* 2007, **23**, 10644.
4 T. Tsoufis, G. Tuci, S. Caporali, D. Gournis, and G. Giambastiani, *Carbon* 2013, **59**, 100.
5 I. Pavlidis, T. Vorhaben, T. Tsoufis, P. Rudolf, U.T. Bornscheuer, D. Gournis and H. Stamatis *Bioresours. Technol.* 2012, **115**, 164.
6 J. Wang, Y. Zhao, F.X. Ma, K. Wang, F.B. Wang and X.H. Xia, *J. Mater. Chem. B*, 2013, **1**, 1406.
7 A. Bourlinos, D. Gournis, D. Petridis, T. Szabó, A. Szeri, and I. Dékány. *Langmuir* 2003, **19**, 6050.
8 (a) H. Liu, T. Kuila, N. Kim, B. Ku, J. Lee. *J. Mater. Chem. A,* 2013, **1**, 3739; (b) D. Yu and L. Yai, *J. Phys. Chem. Lett.* 2010, **1**, 467.
9 (a) H. Liu, T. Kuila, N.H. Kim, B-C Ku and J.H. Lee, *J. Mater. Chem. A* 2013, **1**, 3739; (b) O.C. Compton, S. Kim, C. Pierre, J.M. Torkelson and S.T. Nguyen, *Adv. Mater.* 2010, **22**, 4759.
10 (a) X. Xu, C. Song, J.M. Andrésen, B.G. Miller, A.W. Scaroni, *Micropor. Mesopor. Mat.* 2003, **62**, 29; (b) N. Gargiulo, A. Peluso, P. Aprea, F. Pepe and D. Caputo, *J. Chem. Eng. Data* 2014, **59**, 896; (c) X. Xu, C. Song, J.M. Andresen, B.G. Miller and A.W. Scaroni, *Energy Fuels* 2002, **16**, 1463.
11 L. Estevez, R. Dua, N. Bhandari, A. Ramanujapuram, P. Wang and E. P. Giannelis, *Energy Environ. Sci.* 2013, **6**, 1785.
12 A. Kontos, V. Likodimos, C. Veziri, E. Kouvelos, N. Moustakas, G. Karanikolos. G. Romanos and P. Falaras, *Chem. Sus. Chem.* DOI: 10.1002/cssc.201301323.
13 P. D. Vaidya, E. Y. Kenig, *Ind. Eng. Chem. Res.* 2007, **30**, 1467.